10

# Preparation and Characterization of PVDF/PMMA/Graphene Polymer Blend Nanocomposites by Using ATR-FTIR Technique

Somayeh Mohamadi
*Polymer group,*
*School of Chemistry,*
*University College of Science,*
*University of Tehran, Tehran*
*Iran*

## 1. Introduction

With improvement in the human life, the requisite of the new materials with special properties for many different applications ranging from food packaging and consumer products to use as medical devices and in aerospace technologies can be sensed, strongly. Polymeric materials offer this opportunity to scientists and engineers for designing these new materials. In this regard, precise understanding of Structure and Properties Relationship (SPR) should be very crucial.

Recently, polymeric nanocomposites have opened a new research area and attracted strong attentions. The synthesis of polymer nanocomposites by inserting the nanometric inorganic compounds is an integral aspect of polymer nanotechnology (A. Lagashetty, 2005). These materials, depending upon the inorganic materials present, have particular and improved properties respect to pure polymers that invest their applications.

Fourier transform infrared (FTIR) spectroscopy is a powerful and reliable technique that for many years has been an important tool for investigating chemical processes and structures. In the polymer fields, FTIR data is used in order to study characterization of chemical bonds, polymer microstructure, chain conformation, polymer morphology, crystallinity and etc, consequently is useful in SPR studies.

The combination of infrared spectroscopy with the theories of reflection has made advances in surface analysis possible. Attenuated Total Reflectance (ATR) spectroscopy is an innovative technique for proving chemical information of a sample surface and the ability to quantify newly formed species, based upon Fick's second law. The fundamentals of attenuated total reflection (ATR) spectroscopy date back to the initial work of Jacques Fahrenfort and N.J. Harrick, both of whom independently devised the theories of ATR spectroscopy and suggested a wide range of applications. The schematic showing ATR-FTIR configuration is illustrated in Fig. 1 (KS. Kwan, 1998). The penetration depth, d, can be estimated as:

$$\boldsymbol{d = \frac{1}{2\pi n_c \sigma (sin^2\theta - n_x^2)^{1/2}}} \quad (1)$$

where $n_c$ is the refractive index of the ATR crystal and $n_x$ is the ratio between the refractive indexes of the sample and the ATR crystal ( $si$which both of them are assumed to be constant in the considered frequency range. $\sigma$ is the wave number and $\theta$ is the incident angle. The penetration depth for PVDF as an example by rhe assumption of $n_c = 2.4$, $n_x = 1.5$ and $\theta = 45^{\circ}$ from 500 to 4000 $cm^{-1}$ is approximately 0.5-4 μm (Y. Jung Park, 2005).

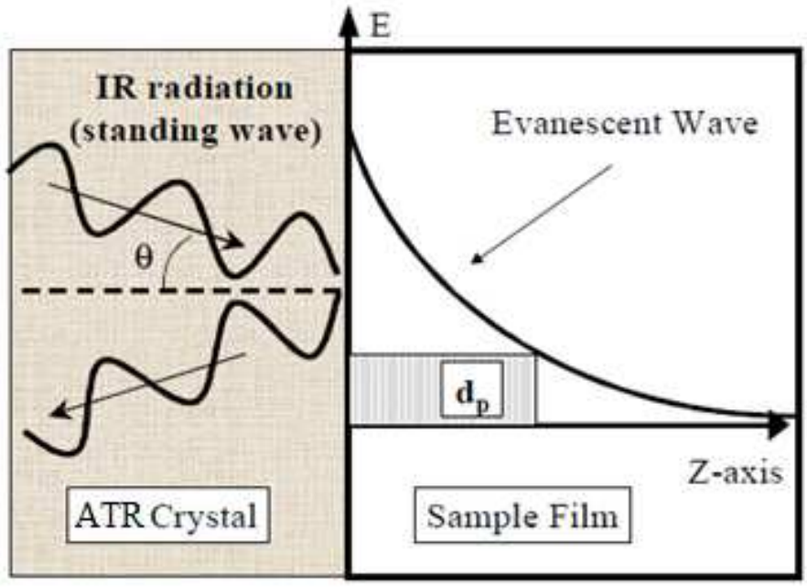


Scheme 1. Schematic illustration of ATR-FTIR configuration (KS. Kwan, 1998)

Graphene and graphite have recently attracted strong attention as versatile, environmentally friendly and available carbon materials which can be used as inexpensive filler in the composite materials (S. Stankovich, 2006, 2007 & L. Al-Mashat, 2010) .Crystalline graphites are used in polymeric systems in order to improve polymer properties such as thermal and electrical conductivity, IR absorption, flame retardancy, barrier resistance, electromagnetic shielding, lubrication and abrasion resistance. When the crystalline graphite is exfoliated to individual graphene sheets, the specific surface would be as large as 2600 $m^2 . g^{-1}$ and novel electronic and mechanical properties appeared (Steurer, 2009). Actually graphene sheets are one-atom two-dimensional layers of $sp^2$- network carbon that their fracture strength should be comparable to that of carbon nanotubes with similar types of defects (S. Stankovich, 2007). How to exfoliate the flakes of natural graphite was first described in a US patent in 1891 (Inagaki, 2004). An exfoliation phenomenon was studied mostly and occurs when the graphene layers are forced apart by the sudden vaporization or decomposition of intercalated species (E. H. L. Falcao, 2007).

However, the mentioned properties of graphene-polymer nanocomposites are strongly dependent on the uniformly dispersion in polymeric matrices which is affected by functional groups present on the graphene surface.

The modification of graphene sheets via organic oligomeric and polymeric chains is a favorable way to promote the compatibility of these nanoparticles with polymeric media. So understanding of the functional groups present on the graphene surface should be very vital for designing of modification procedure.

Poly(vinylidene fluoride) (PVDF) is a semicrystalline engineering polymer with very good resistance to chemicals, oxidation, and UV radiation (J. H. Yen, 2006). PVDF is known for its polymorphism crystalline structure and complicated microstructure. It is one of the most widely studied polymers due to its non-linearity, piezo- and pyro-electricity (L. T. Vo, 2007 & K. Pramoda, 2005). PVDF can crystallize in at least five well-known crystalline phases (E. Giannetti, 2001, A. Lovinger, 1982 & N. S. Nalwa, 1995):

α and δ with conformation of the alternating trans-gauche ($TG^+TG^-$) which the α is the most common form and is the most thermodynamically stable.

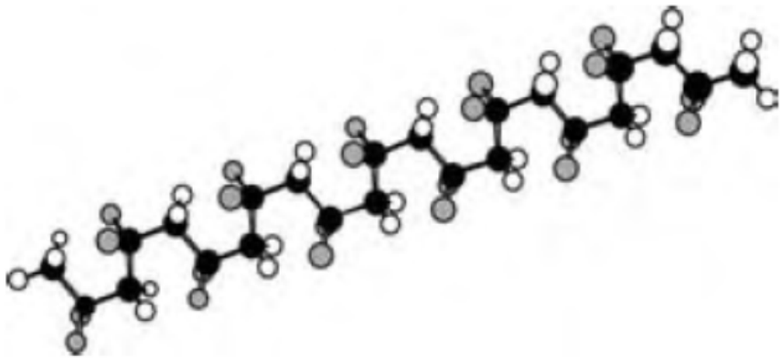

Scheme 2. α and δ form with alternating trans-gauche conformation (J. H. Yen, 2006)

β with all trans (TTT) planer zigzag conformation is polar form and has been extensively studied for its potential applications. This form develops under mechanical deformation (K. Matsushige, 1980) (S. Ramasundaram, 2008) , growth from solution (J. Wang, 2003 & R. L. Miller, 1976), addition of metal salts (X. He, 2006 &W. A. Yee, 2007) ,melt crystallization at high pressures (D. Yang, 1987), application of a strong electric field (J. I. Scheinbeim, 1986), blending with carbonyl-containing polymers (C. Lbonard, 1988 & K. J. Kim, 1995), and recently, addition of nanoparticles (S. Ramasundaram, 2008, T. Ogoshi, 2005 & L. He, 2010). This structure provides some unique properties for PVDF piezo- and pyro-electric activity:

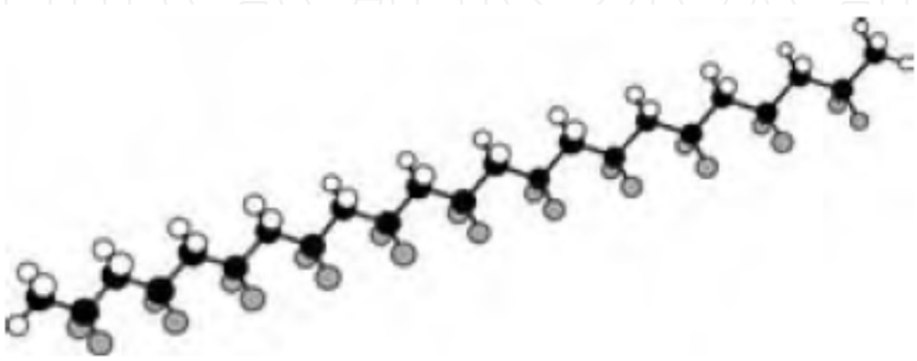

Scheme 3. β form all trans planer zigzag conformation (J. H. Yen, 2006)

γ and ε with $T_3G^+T_3G^-$ conformation is also polar but less than β form.

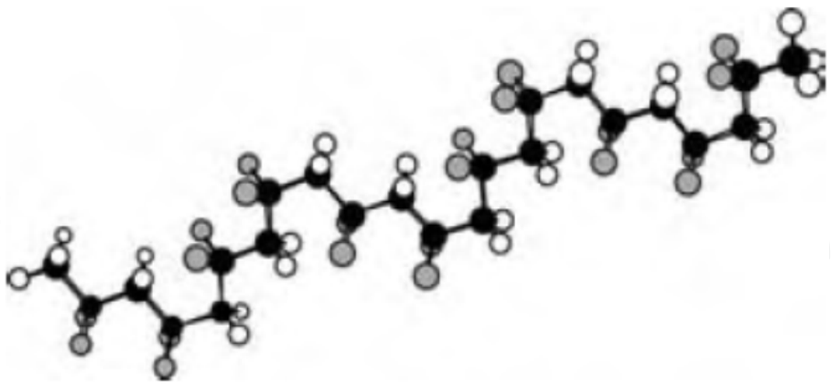

Scheme 4. γ and ε crystalline form with $T_3G^+T_3G^-$ conformation (J. H. Yen, 2006)

Subsequently due to specific chain conformation in crystal unit cell and providing the highest remnant polarization, β phase has attracted more attention than the others in pyro- and piezoelectric applications (J.Jungnickel, 1996).

Poly methylmethacrylate (PMMA) can interact with graphene sheets by the interaction of delocalized π-bonds of graphene with π-bonds of PMMA. On the other hand, as reported in articles, PVDF/PMMA blend is a miscible system. Consequently, in attempt to achieve a homogenous dispersion of nanographene layers in PVDF matrix, the use of PMMA chains as a compatiblizer can be useful.

In addition, presence of PMMA chains in the close touch with PVDF molecules causes the formation of polar crystalline form in PVDF (J. Wang, 2003). Furthermore, previous studies on the CNTs indicated TTT molecular chain prefers to be absorbed on the CNT surface compared with TGTG' molecular chain, and the configuration in which H atoms and CNT surface are face-to-face are more stable than that where F atoms and CNT surface are face-to-face. Since in the PVDF, the negative charge transfer from H to C atom and the negative charge is accumulated around the F atoms, the interaction between the H atoms with positive charge in PVDF and C atoms with π oribital in CNT should be stronger (S. Yu, 2009)

FT-IR is a powerful and reliable technique for description of chemical characterization of graphene and also study of the structure and properties relationships in PVDF/PMMA/graphene polymer blend nanocomposite. The interactions between these three components including: PVDF, PMMA and graphene sheets can be revealed and described by using this technique. As well, exploration of PVDF chains conformations (crystalline structures) are affected by presence of graphene sheets and PMMA chains can be done which is very important in order to design the new material with special properties.

## 2. Experimental

### 2.1 Materials

The graphite used in this study was natural graphite powders with the size of >150 μm, and bulk density of 1.65 gr/cm3 supplied by Iran Petrochemical Co. The PVDF pelletlet (Kynar®

1000HD) was provided by Atofina Co. The methyl methacrylate (MMA) and Methacyilic anhydride were supplied by Aldrich Co. and MMA used after purification and distillation in order to remove inhibitors. Concentrated sulfuric acid and nitric acid with concentration of 63% were used as chemical oxidizer to prepare expanded graphite. The initiator, Benzoyl peroxide (BPO), dichloromethane ($CH_2Cl_2$), dimethylformamide (DMF), triethylamine (TEA) were bought from Merck Co. and used as received.

### 2.2 Preparation of exfoliated graphite

The method which was used in this study is as same as general procedure employed in industry for producing exfoliated graphite. Natural graphite powders as starting material were treated with a mixture of 4:1 sulfuric and nitric acid at 80°C for 24h to produce Graphite Intercalated Compounds (GIC)s. Graphite can accept many species into the gallery between graphite layer planes to form GICs.

Sulfuric acid is the most conventional intercalate for achieving a high degree of exfoliation of natural graphite and so it is used most commonly in the industry. Nitric acid was also added as an oxidant to generate some functional groups such as hydroxyl, carboxyl, epoxid groups on the surface and edge of graphene sheets.

The suspension of acid-treated graphite was added to excess distilled water, and this was followed by centrifugation with 5000 rpm and washing with water until the pH of the centrifuge drainage extraction was natural.

These particles dried at oven at 100°C for 12h and vacuumed oven at 80°C for 8h. The oxidized graphite was heat-treated at 1050 °C for 45s to obtain expanded graphite. Actually, In Chung's review, exfoliation phenomena were classified into reversible and irreversible ones. When the oxidized graphite was heated to around 300°C,it expanded to a fractional expansion of about 30 and upon cooling collapsed, again. This expansion–collapse phenomenon was reversible, and was thus called reversible exfoliation.

But if it is heated to a higher temperature (e.g., 1000°C), the intercalating compound and some of functional groups decompose completely and at the same time the host graphite flakes exfoliate up to about 300× in volume, particularly by rapid heating. This exfoliated graphite never returns to the original thickness upon cooling to room temperature, that is, we have irreversible exfoliation. The expanded graphite was immersed in absolute ethanol and sonicated for 30 min in order to exfoliate and break down to individual layers. The dispersion was filtered and dried at oven at 80°C for 8h and vacuumed oven at 80°C for 4h to remove residual moisture in the graphite particles (S. Mohamadi N. S.-S., 2011).

### 2.3 Modification with methacrylic anhydride

The above Functionalized Graphite, which is called FG, was reacted with methacrylic anhydride to provide some organic groups and vinyl moieties on the surface of graphene. Actually, the functional groups which were introduced in the previous process could further react with methacrylic anhydride through hydroxyl groups. A 250-mL flask was charged with 100 mL of DMF, 10 mL TEA and 100 mg FG and after sonication for 30 min, a solution of containing 5 mL methacrylic anhydride and 90 mL DMF was added in to the mixture.

This mixture was allowed to react at 90°C for 24h under magnetic stirring. After that the Modified Graphite, for simplicity it is called MG, were collected by filtration and followed by thorough washing with distilled water to remove any residual TEA and then washed with $CH_2Cl_2$, in order to remove any unreacted methacrylic anhydride. The washed particles were dried in oven and vacuum oven at 80°C for 8h, separately.

### 2.4 Preparation of PMMA/ graphene masterbatch

The PMMA-graphene masterbatch (PMMA-G master) was prepared via polymerization of MMA with BPO as an initiator. 300 mg of MG was dispersed in 15 mL MMA via ultrasonication for 30 min. The polymerization was initiated by (1.1% wt) of BPO respect to monomer in flask at 90°C, until the polymerization was solidified, completely. Later then, the prepared masterbatch was kept in vacuum oven at 120°C to remove any remaining MMA. The content amount of graphite was kept in 2.5 wt%.

### 2.5 Preparation of PVDF/PMMA/graphene nanocomposite

PVDF and PMMA-G master solutions were prepared separately by dissolving in DMF at 50°C with stirring for 1 day. Both of the resulting solutions were blended, so that the final concentration of mixture adjusted in 12% wt. on the weight of PVDF/PMMA-G master respect to solvent. The mixture was sonicated for about 30 min, stirred 2 days and spread on a well-cleaned glass slide of petridish. The prepared sample was carefully evaporated at 60°C in an oven for 20 h and then divided into three parts and annealed at three different temperatures of 50, 90 and 120°C in vacuum oven for 24 h. three samples with varying PVDF/PMMA-G master ratios of 80:20, 70:30 and 60:40 were prepared and analyzed. For convenience the samples were named as 80:20, 70:30, 60:40 and 70:30 No G, respectively (S. Mohamadi, 2011).

### 2.6 Characterization

The Fourier transform infrared (FT-IR) analysis was performed on a Bruker Equinox55 Analyzer, equipped with a DTGS detector and a golden gate micro ATR from 600 –3500 $cm^{-1}$. Scanning electron microscopic (SEM) and TEM images were obtained on a Zeiss CEM 902A (Oberkochen, Germany) and Philips-CM-120, Netherlands at an accelerating voltage of 120 KV, respectively. The thermal behavior was measured with a DSC Q100 from the TA instruments with the heating and cooling ramp of 10 $^oC$ min-1 from room temperature to 250 $^oC$ under argon flow. The X-ray diffraction (XRD) patterns of the samples were recorded by Philips, Netherlands advanced diffractometer using Cu(Kα) radiation (wavelength: 1.5405Å) at room temperature in the range of 2θ from 4 to 70° with a scanning rate of 0.04°. $S^{-1}$.

## 3. Results and discussion

As reported by others in several literatures, presence of the relatively broad peak at 3427 $cm^{-1}$ and also the peak at 1402 $cm^{-1}$ in the FTIR spectra of graphite oxide indicate existence of hydroxyl groups. In addition, the peaks at 1720, 1640, 1580 and 1060 $cm^{-1}$ can be assigned to the stretching vibration of carboxyl, carbonyl moiety of quinine, aromatic C=C bonds and epoxide groups, respectively (scheme 1) (C. Hontoria-Lucas, 1995) . To determine which

functional groups existed in the graphene sheets after heat treated of graphene oxide (FG) and functionalization with methacrylic anhydride, the related FTIR spectra has been illustrated in Fig. 1.

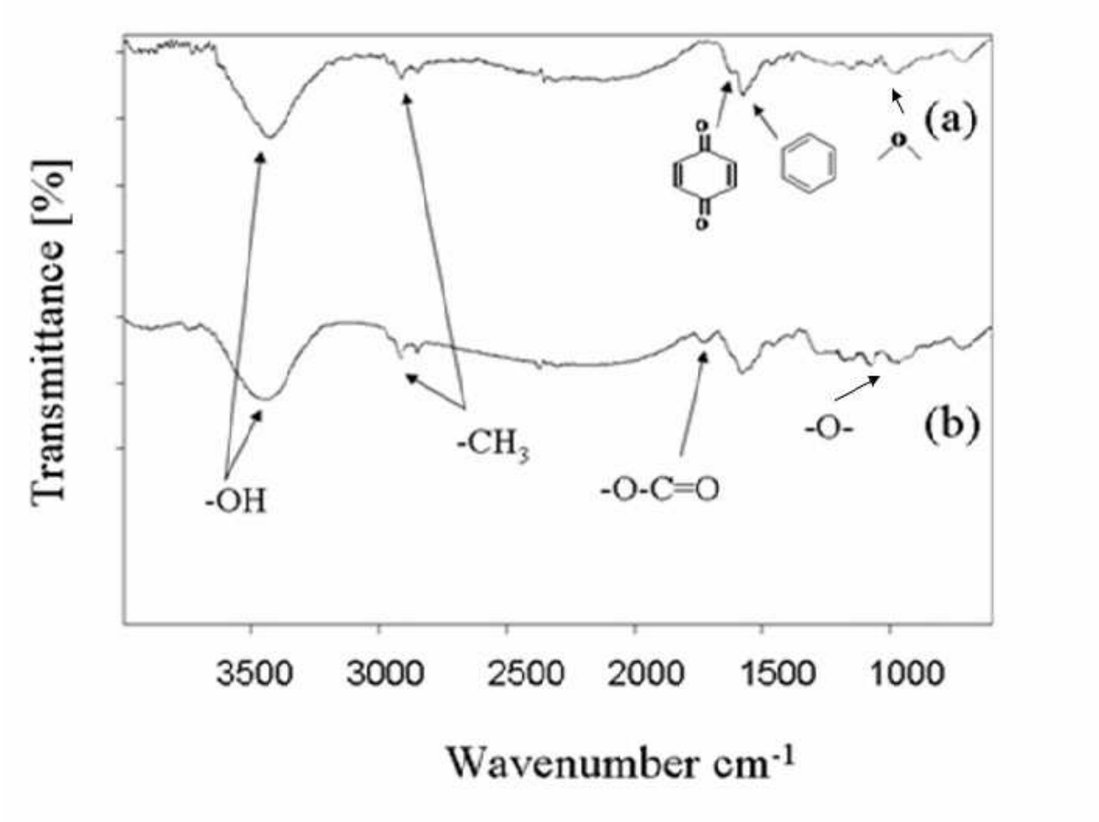


Fig. 1. FTIR spectrums of FG (a) and MG (b).

As can be seen in Fig. 1 (a) most of carboxyl groups in the graphene oxide has decomposed during heat-treatment of graphite oxide so that the peak at 1720 $cm^{-1}$ disappeared. In fact, during the acid treatment various oxygen-functional groups were produced on the graphene surface. While, in the heat-treatment step, the oxygen containing of graphene was reduced but some introduced functional groups remained and still the particles can contain significant amount of oxygen (Steurer, 2009).

In addition, the peaks at 2960 and 2930 $cm^{-1}$ are related to the asymmetric and symmetric stretching vibration of pendant methyl groups. Symmetric vibrations are generally weaker than asymmetric vibrations since the former lead to less of a change in dipole moment. Actually, during sonication it may graphene flakes are broken and this pendant methyl groups came into sight.

In the case of MG, (Fig. 1 (b)) appearance of a new peak at 1740 $cm^{-1}$ which has been assigned to vibration of esteric carbonyl group is due to the formation of esteric linkages between hydroxyl groups of FG and methacrylic anhydride (Scheme 6). Modification of FG by methacrylic anhydride (MG), causes appearance of the new methyl groups which show the peaks at 2960 and 2930 $cm^{-1}$. Furthermore, C=C band at 1580 $cm^{-1}$ has become

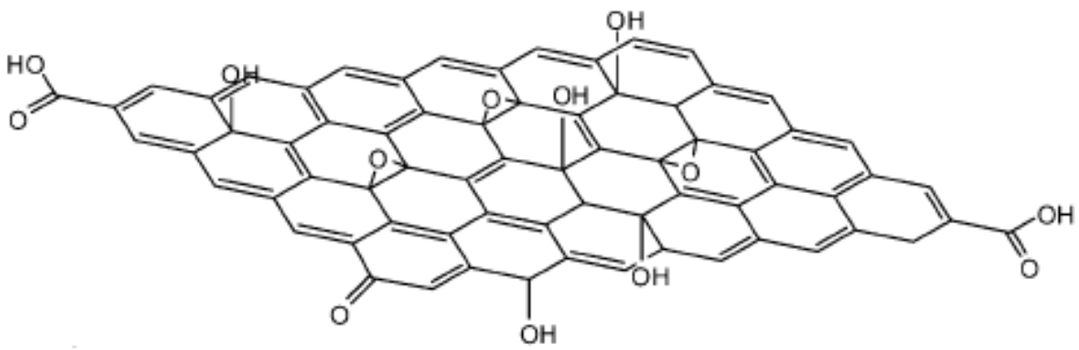


Scheme 5. Graphite oxide (P. Steurer, 2009)

more broader in MG rather than FG may due to presence of aromatic and aliphatic double bonds.

ATR-FTIR spectrum of pure PVDF film which was annealed at 50°C, from 550-3500 $cm^{-1}$ is also shown in Fig.2. The observed pattern originates from oscillations of large parts of the skeleton and/or the skeleton and attached functional groups. Below 1500 $cm^{-1}$, most single bonds absorb at similar frequencies, and the vibrations couple.

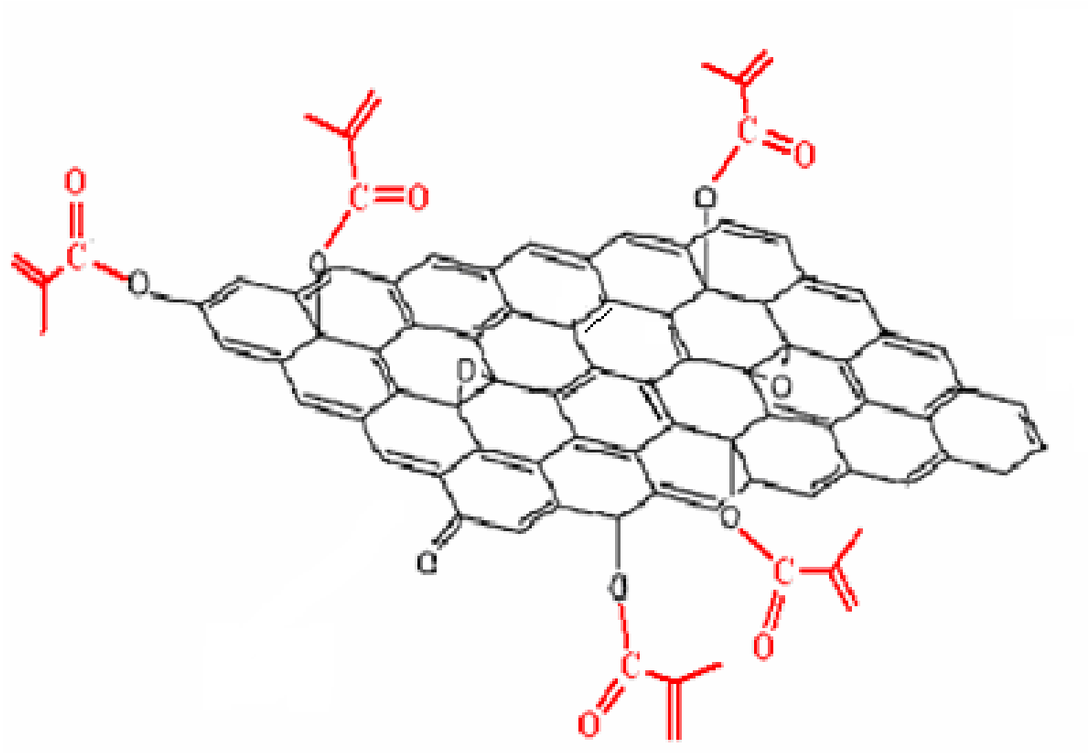


Scheme 6. Modified graphen with methacrylic anhydride (S. Mohamadi, 2011)

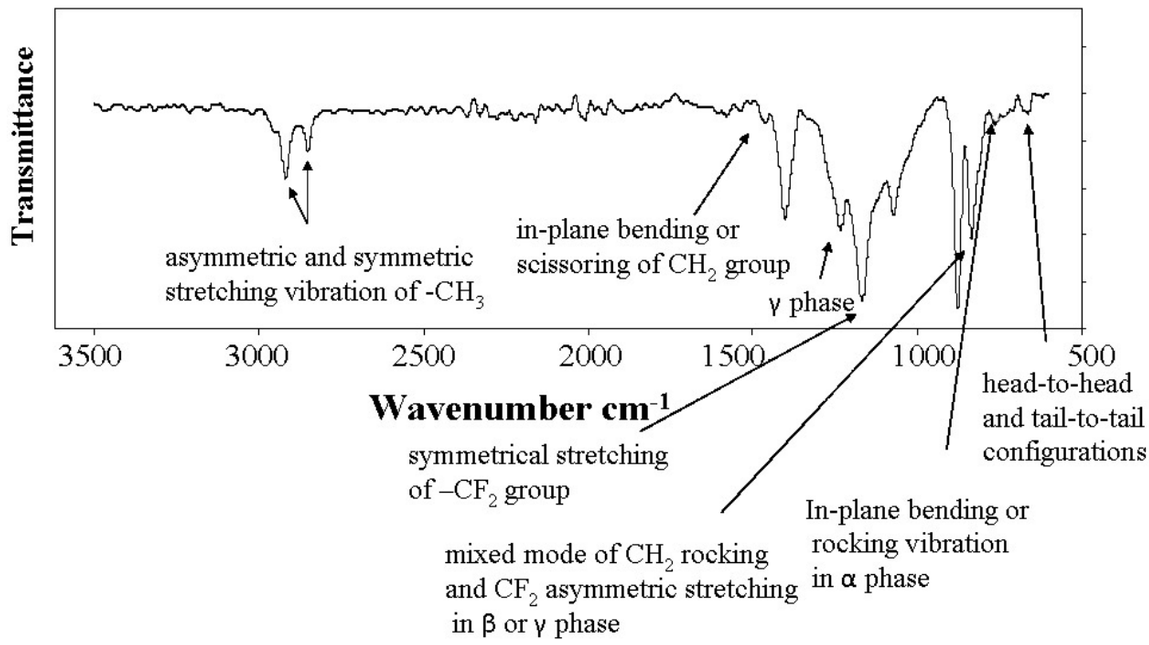


Fig. 2. ATR-FTIR spectrum of pure PVDF film which was annealed at 50°C

It should be pointed that since the β- and γ-phase are similar to each other in short segmental conformations the identification of crystal phase between β and γ in FTIR spectrum is still in dispute. On the basis of the data from literature the absorption band at 763 $cm^{-1}$ is related to In-plane bending or rocking vibration in α phase (N. Betz, 1994 & S. Lanceros-Me ndez, 2001), the band at 840 $cm^{-1}$ stretching in β or γ phase (G. Chi Chen, 1994 , V. Bharti, 1997, B. Mattsson, 1999 & M. Benz, 2002), the band at 1173 $cm^{-1}$ is associated to the symmetrical stretching of $–CF_2$ group (M. Rajendran, 2010). The band at 1234 $cm^{-1}$ is related to the γ phase and 1453 $cm^{-1}$ is assigned to in-plane bending or scissoring of $CH_2$ group (M. Rajendran, 2010 & Garton, 1992).

In addition, some irregularities of head-to-tail addition, leading to defect structures, can occur during polymerization for several reasons in polymers of the vinylidene class, sequence isomerism may occur. The transmission band at 677 $cm^{-1}$ points to the presence of head-to-head and tail-to-tail configurations (B. Hilczer, 1998). Such defects are produced during the polymerization process and reduce the dipole moment of the all-trans conformation.

Fig. 3 shows ATR-FTIR spectra for pure PVDF film (a), G-PMMA master (b), 80:20 (c), 70:30 (d), 70:30 NoG (e), 60:40 (f) which were annealed at 50°C from 550-2000 $cm^{-1}$. When MG was incorporated in PMMA matrix (G-PMMA master), the absorption originating from MG particles alone were hardly visible. G-PMMA master spectrum clearly shows several characteristic peaks at 1723, 1449 and 1142 $cm^{-1}$ which are related to the presence of PMMA chains, assigned to ester carbonyl (C=O), $O–CH_3$ and C-O (ester bond) stretching.

Polymer- polymer interactions may also affect PVDF chain conformations. Specific interactions are very sensitive to the distance between the interacting groups and to their

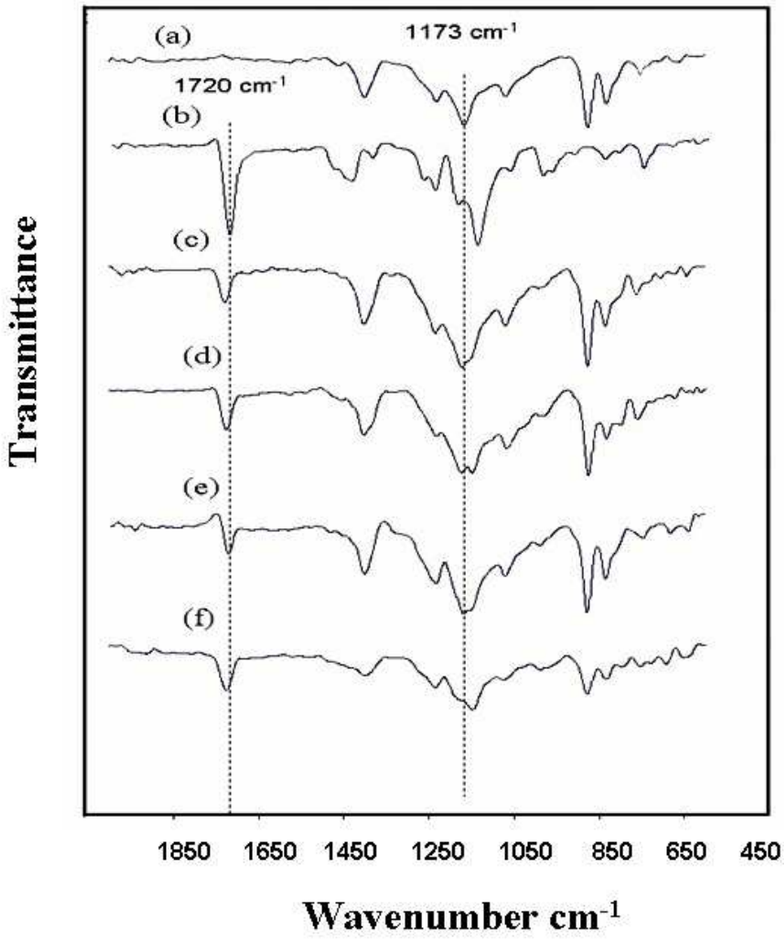


Fig. 3. ATR-FTIR spectra of pure PVDF (a), G-PMMA master (b), 80:20 (c), 70:30 (d), 70:30 NoG (e), 60:40 (f) which were annealed at 50°C.

relative orientation: hydrogen bonding strength falls off rapidly when the atomic distance increases or when the bond is bent instead of linear. This infers that the efficiency of the contact between two unlike chains depends on their respective conformation (eventually tacticity) and flexibility. The chains are expected to adopt an optimate conformation for interacting (C. Lbonard, 1988).

To identify the nature of the interactions in the polymer blend nanocomposite, we choose the band at 1720 $cm^{-1}$ which is due to the stretching vibration of the C=O group in PMMA as a characteristic peak of PMMA. This band shows a little shift to the higher frequencies and has become broader in both of the polymer blend with no graphen and nanocomposites. These changes can be ascribed by the interaction between PMMA and PVDF chains (I. S. Elashmawi, 2008 & M. M. Colemann, 1995).

The strong absorption peak which appeared at 1173 $cm^{-1}$ is assigned to the symmetrical stretching of $-CF_2$ groups, was choose as characteristic peak of PVDF in polymer blend nanocomposites. The precise consideration reveals shifting of this band to the higher frequencies in the synthesised samples comparing to pure PVDF. Since this shifting is

slighter for 70:30 NO G than polymer blend nanocomposites, it can be imagined this change is related to the specific interactions between PVDF and graphene surface in the nanocomposites. Also, it can be concluded GNPs increase the compatibility of PVDF and PMMA.

On the other hand as mentioned above, presence of polymer-polymer interactions can also affect the polymer conformations. PVDF exhibits short bond sequences tt and tg; the probability of a gg bond is negligible because of steric hindrance. Energy calculations emphasize that PMMA conformation remains close to all trans conformation of PVDF. In our study, presence of graphene particles along with PMMA chains makes it complex due to PVDF-PMMA, PVDF-graphene and PMMA-graphene interactions.

The surface morphology of the casted films was studied using SEM analysis. In each sample, the surface which is exposed to the air is examined. The distinguishable spherulitic structure on the top surface of pure PVDF film could be seen which had extended from 9 μm to about 15 μm with increasing the annealing temperature from 50 to 120°C. But in 70:30 some new elongated ribbon like crystals on the spherulitic structures can be observed which became more visible with increasing annealing temperature to 120°C (Fig. 4). Y. J. Park et al reported the oriented align crystalline PVDF lamella which has bamboo-like structure can be achieved when PVDF film casted from polar solvent such as DMF and DMSO and crystallize in the confined spaces of the specific mold at high temperature. In their view, these structures are due to the formation of γ crystals (Y. J. Park, 2005).

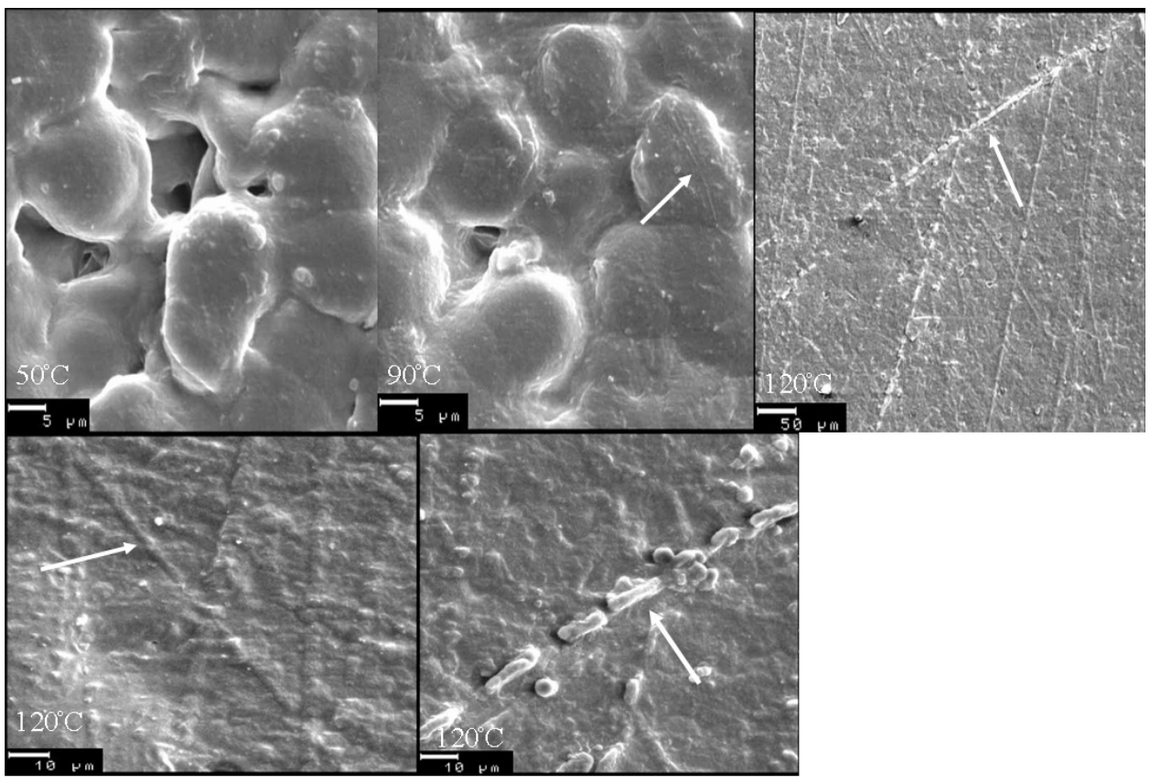


Fig. 4. The surface morphology of the casted 70:30 film were annealed at 50, 90 and 120°C.

We analyzed ATR-FTIR spectrum of 70:30 sample which were annealed at 50, 90 and 120° C (Fig. 5). From the previous reports on the spectral features of each crystal phase in PVDF, two IR absorptions band at 762 $cm^{-1}$ and 1234 $cm^{-1}$ as the representative of α- and γ-phase were selected to compare the peak intensities in each annealed samples.

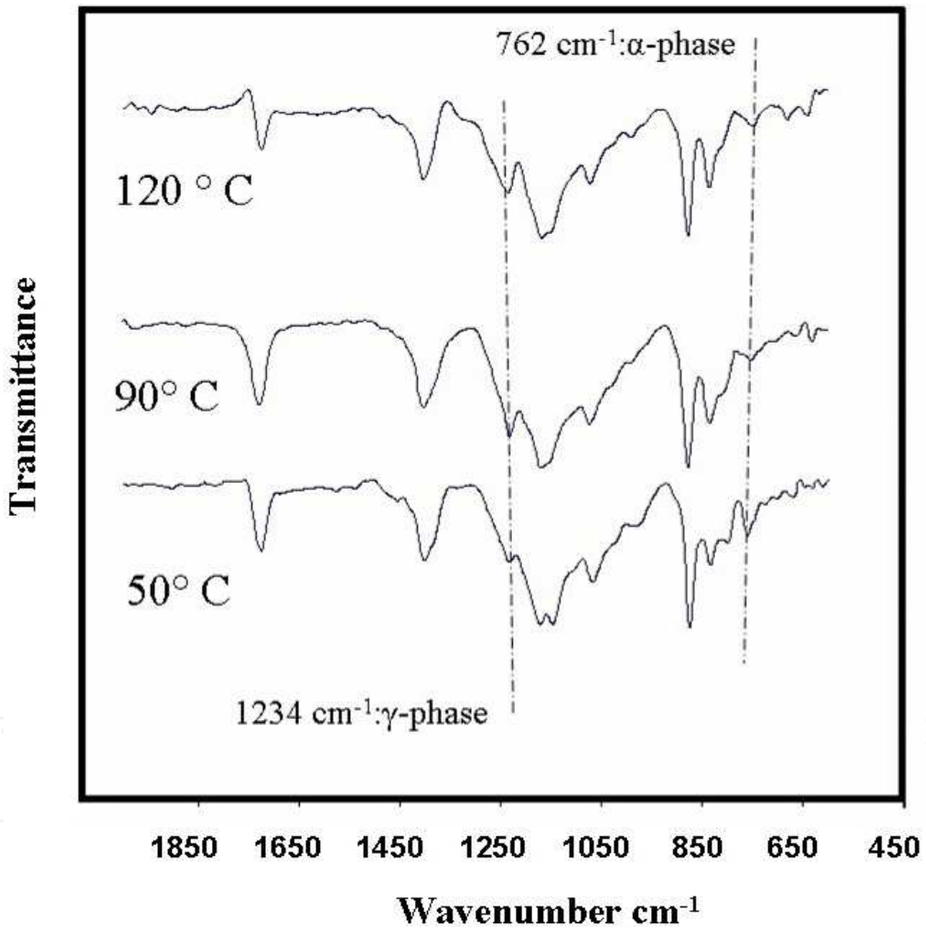


Fig. 5. ATR-FTIR spectra of 70:30 were annealed at 50, 90 and 120° C.

It indicated with increasing annealing temperature the percentage of γ-phase on the surface increased while α-crystal decreased at 90° C and then didn't change significantly, at 120°C. In this regards, this new droplet like structure identities on the top of the films can be related to γ-phase. Of course, this result is in agreement with X-ray Diffraction (XRD) and Differential Scanning Calorimetery (DSC) results (Fig. 6).

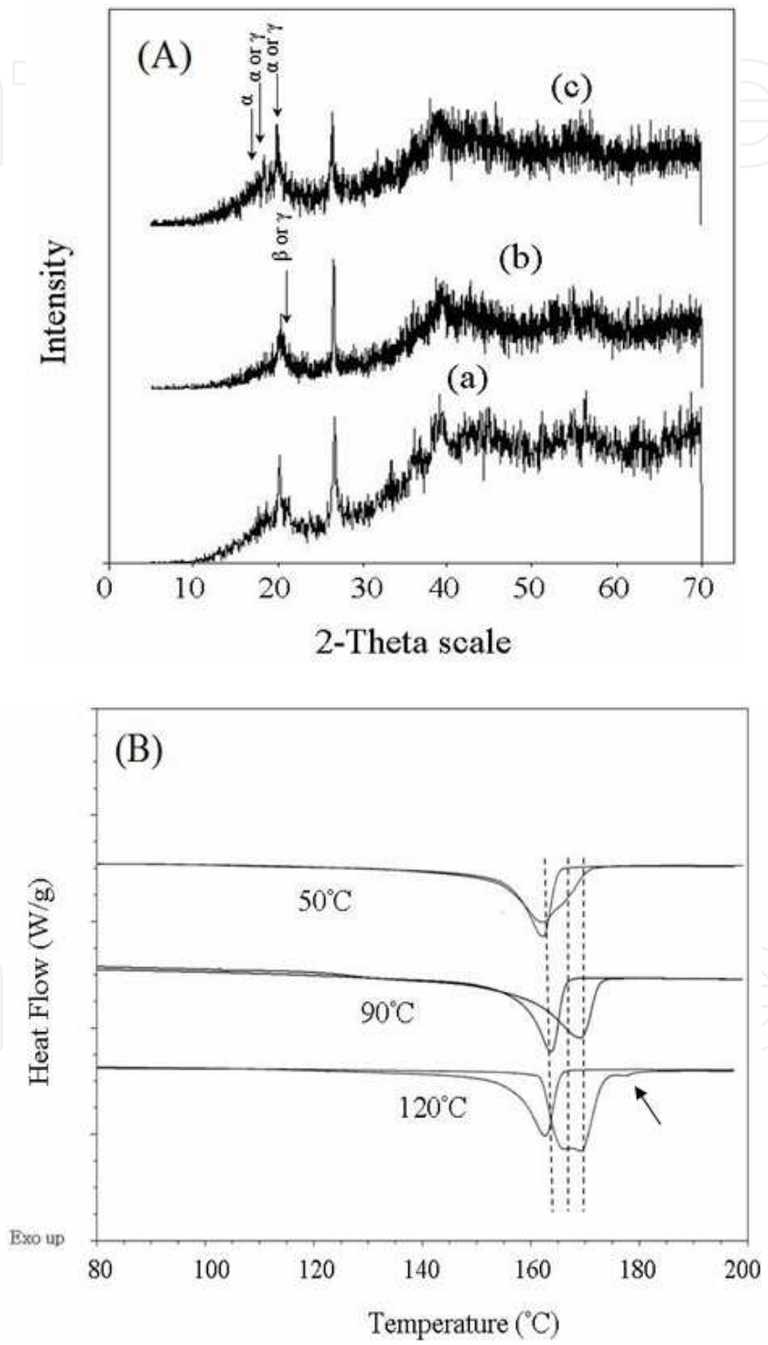


Fig. 6. X-ray diffraction pattern (A) and DSC thermograms of first and second heating (B) of 70:30 films annealed at 50, 90 and 120°C for 24h (S. Mohamadi, 2011)

On the basis of the reported data in literatures, WAXD data of neat PVDF contain 100, 020, 110, 021 reflections at 2θ= 17.9°, 18.4°, 20.1°, and 26.7° for α- and only 200/110 reflection at 2θ= 20.8° for β-crystalline form (A. Kaito, 2007, L.Yu, 2009 & G. Guerra, 1986). γ-crystal planes are known to have overlapping reflections with (020), (110) and (021) α-crystal planes and also 200/110 reflection of β-phase. The (100) peak of α- phase at 2θ= 17.9° is the only peak that doesn't have any overlapping with γ-phase. Also the sharp diffraction peak at 26.38° in 70:30 is related to the crystallographic plane of graphite with d-spacing of 3.37Å, indicating that the graphite retained its crystalline structure in nanocomposite but there is a different degree of stacking order and disordered microstructure (K. P. Pramoda, 2010 & T. Ramanathan, 2007). Furthermore, the film which was annealed at 50°C shows the 100, 020, 110 reflections of α-phase and 200/110 reflection of β-crystal In XRD pattern of the films were annealed at 90°C, 200/100 reflection of β-crystal has become stronger, while the 100 peak of α has not changed considerably. It means with increasing temperature to 90°C, the growth of β-crystals is more favorable than α-crystals. Increasing the annealed temperature to the 120°C caused the substantial variation in the intensity of reflections. The decrease in the intensity of 200/100 reflection of β-crystal and increase in 020, 110 reflections of α- or γ-phase without any significant change in 100 reflection of α-crystal implies some of β-crystals convert to γ-crystals at 120°C. The DSC results also matched well with those of X-ray diffractions and indicated the existence of the different types of crystal structures. The new appeared endotherm in the film which was annealed at 177° C can be attributed to the melting of the new formed ribbon-like structures on the surface.

Actually, in our work, it can be imagined PVDF chains which are trapped between graphen sheets and are in close contact with PMMA chains, crystallize in the confined spaces that are provided by graphen sheets and PMMA chains. It is demonstrated that exfoliated graphene-based materials are often compliant, and when dispersed in a polymer matrix are typically not observed as rigid disks, but rather as bent or crumpled platelets (J. R. Potts, 2011). Consequently, as can be seen in TEM image of 70:30 sample (Fig. 7), the wrinkled surface of

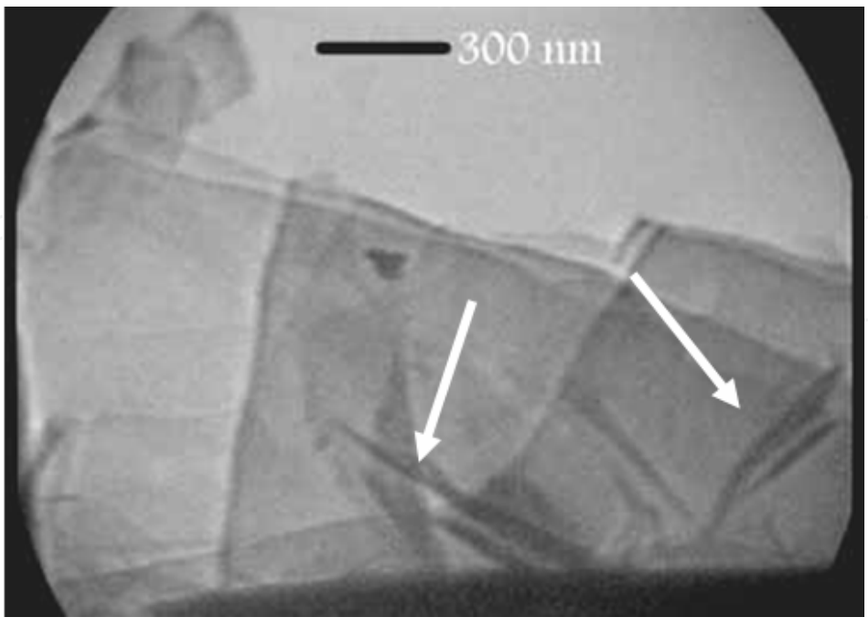


Fig. 7. TEM image and Wrinkled surface of graphene sheets in 70:30 polymer blend nanocomposite (S. Mohamadi, 2011)

the graphene sheets can act as micropattern molds for crystallization of PVDF. In other words, a well-defined feature of micropattern can be provided by the wrinkles on the surface of graphene sheets.

Crystallization results basically in the succession of two events: the primary nucleation of a new phase and then the three-dimensional growth of lamellae; these steps can be followed by lamellar thickening, fold surface smoothing, or reorganization into more perfect crystals. As reported by others, with increasing the annealing temperature in PVDF/PMMA blend film, the amount of α phase increases due to easier local internal chain rotation at higher temperature and most of β and γ form convert to α form.

While in our study with increasing the annealing temperature the amount of α phase decreased and γ form increased. It can be said graphene sheets can stabilize the β- and γ-phase at elevated temperature due to restricting effect of graphene sheets on TT conformation chains as is illustrated in scheme:

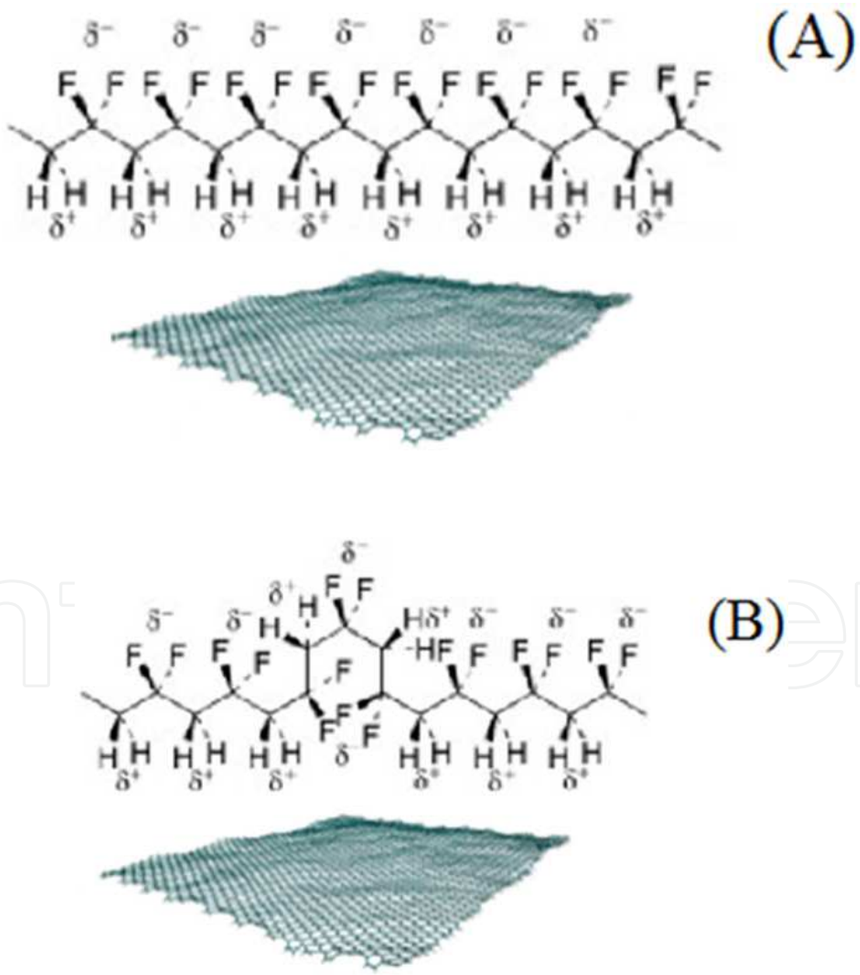


Scheme 7. Schematic illustration of to restricting effect of graphene sheets on TT (A) and $TTTG^{+}TTTG^{-}$ (B) conformation chains

## 4. Conclusion

In this study, modification of graphite was carried out via introduction of hydroxyl groups and then vinyl groups on the surface of graphite by oxidation and estrification reaction respectively. The modified graphene (MG) was used to prepare the PMMA-graphene as a master batch by in-situ polymerization and followed by solution blending with PVDF in different ratios. The series of prepared polymer blend nanocomposite films were annealed at three different temperatures of 50, 90 and 120°C, and characterized.

FTIR results for FG and MG confirmed presence of different oxygen containing function groups on the surface of FG and vinyl organic moieties on the MG sheets.

ATR-FTIR spectra revealed the specific interaction between PVDF and PMMA chains in polymer blend nanocomposites. The surface morphology of 70:30 film which was annealed at 120˚C, some new elongated ribbon like crystals formed. From ATR-FTIR data of this sample the identity of these new structures on the film surface can be related to the formation of γ crystals.

## 5. Acknowledgment

We are thankful to the Research Council of the University of Tehran. We gratefully acknowledge the kind assistance from Ms. Fotouhi from the thermal analysis laboratory of the University College of Science at University of Tehran for DSC analyses. The authors would also like to thank Dr. Saeed Sepehriseresht from Tehran Heart Center for TEM analyses and helpful recommendations.

## 6. References

Al-Mashat, L., Shin, K., Kalantar-zadeh, K., D. Plessis, J., H. Han, S., W. Kojima, R., B. Kaner, R., Li, D., Gou, X., l J. Ippolito,S. & Wlodarski, W., (2010) Graphene/Polyaniline Nanocomposite for Hydrogen Sensing, Journal of Physical chemistry C, Vol. 114, pp. 16168–16173, 1932-7447.

Benz, M., Euler, W. B., & Gerory, O. J., (2002) The Role of Solution Phase Water on the Deposition of Thin Films of Poly (vinylidene fluoride), *Mocromolecules*, Vol. 35, No. 7, pp. 2682-2688, ISSN 0024-9297.

Betz, N., Le Moel, A., Balanzat, E., Ramillon, J.M., Lamotte, J., & Gallas, J. P., (1994) FTIR Study of PVDF Irradiated by Means of Swift Heavy Ions, *Polymer Science Part B: Polymer Physics,* Vol. 32, pp.1493–1502, ISSN 1099-0518.

Bharti, V., Kaura, & T., Nath, R., (1997) Ferroelectric Hysteresis in Simultaneously Stretched and Corona-Poled PVDF Films, *IEEE Transactions on Dielectrics and Electrical Insulation,* Vol 4, No. 6, (December 1997) pp. 738–741, ISSN 1070-9878.

Chi Chen, G., Su, J., Fina, L. J., (1994) FTIR-ATR Studies of Drawing and Poling in Polymer Bilaminate Films, J. *Polymer Science: Part B, Polymer Physics*, Vol.32, pp.2065-2075, ISSN 1099-0518

Coleman, M. M., Painter. P.C., (1995) Hydrogen bonded polymer blends, *Progress in Polymer Science*, Vol. 20, No. 1, pp.1- 59, ISSN 0079-6700.

Elashmawi, I. E., Hakeem, N.A., (2008), Effect of PMMA Addition on Characterization and Morphology of PVDF, *Polymer Engineering Science*, Vol. 48, pp. 895-901, ISSN 1548-2634.

Falcao, E. H. L., Blair, R. G., Mack, J. J., Viculis, L. M., Kwon, C., Bendikov, M., Kaner, R. B., Dunn, B. S., & Wudl, F., (2007). Microwave exfoliation of a graphite intercalation compound, *Carbon*, Vol. 45, No. 6, pp. 1364-1369, ISSN 0008-6223.

Garton, A., (1992) *Infrared Spectroscopy of Polymer Blends, Composites and Surfaces,* Hanser Publisher, Munich, Germany, ISBN 1-56990-034-5

Giannetti. E., (2001), Semi-crystalline fluorinated polymers, *Polymer International*, Vol: 50, No. 1, ( February 2000), pp. 10-26, ISSN 1097-0126.

Grafting of PMMA Chains Through in-situ Polymerization. Macromolecular Science Part A: Pure & Applied Chemistry, Vol. 48, pp. 577–582, ISSN 1060-1325.

Guerra, G., Karasz, F. E. , Macknight. W. J., (1986), On blends of poly(vinylidene fluoride) and poly(vinyl fluoride), Macromolecules, Vol. 19, No.7, (March, 1986) pp. 1935-1938, ISSN 0024-9297

He, L., Xu, Q., Hua, C., Song. R., (2010) Effect of multi-walled carbon nanotubes on crystallization, thermal, and mechanical properties of poly(vinylidene fluoride, Polymer Composite, Vol. 31, No. 5, ( April 2009), pp. 921-927, ISSN 0272-8397.

He, X. & Yao, K., (2006), Crystallization mechanism and piezoelectric properties of solution-derived ferroelectric poly(vinylidene fluoride) thin films, *Applied Physics letter*. Vol. 89, No. 11, pp. 112909-1 – 112902-3, ISSN 0003-6951.

Hilczer, B., & Kulek. J., (1998) The Effect of Dielectric Heterogeneity on Pyroelectric Response of PVDF, *IEEE Transactions on Dielectrics and Electrical Insulation*, Vol. 5, No. 1, pp. 45–50, ISSN 1070-9878.

Hontoria-Lucas, C., Lopez-Peinado, A. J., DE D. Lopez-Gonzalez, J., Rojas-Cervantes, M. L., & Martin-Aranda, R. M., (1995). Study of oxygen-containing groups in a series of graphite oxides: physical and chemical characterization , *Carbon*, Vol. 33, No. 11, pp. 1585-1592 ISSN, 0008-6223.

Inagaki, M., Kang, F., & Toyoda, M. (2004) Exfoliation of Graphite via Intercalation Compounds in: *Chemistry and Physics of Carbon A Series of Advances* , Radovic, L. R., pp. (1-65) Marcel Dekker, NewYork, ISBN 0-8247-4088-2.

J.Jungnickel, B. (1996). *Polymeric Materials Handbook,* J. C., Salamone, New York : CRC press Inc, . pp. 7115-7122.

Kaito, A., Iwakura, Y., Hatakeyama, K., & Li, Y., (2007) Organization of Oriented Lamellar Structures in a Miscible Crystalline/Crystalline Polymer Blend under Uniaxial Compression Flow near the Melting Temperature, *Macromolecules*, Vol. 40, (February, 2007), pp. 2751-2759, ISSN 0024-9297

Kim, K. J. , Cho, Y. J. , & Kim. Y. H. , (1995) Factors determining the formation of the β crystalline phase of poly(vinylidene fluoride) in poly(vinylidene fluoride)-poly(methyl methacrylate) blends, *Vibrational Spectroscopy*, Vol. 9, No. 2. (September 1994), pp. 147-159, ISSN 0924-2031.

Kwan, KS. (1998) The Role of Penetrant Structure in the Transport and Mechanical Properties of a Thermoset Adhesive, Ph.D. Thesis, Faculty of the Virginia Polytechnic Institute, Blacksburg, 285f.

Lagashetty, A., & Venkataraman, A., (2005) Polymer Nanocomposites, *RESONANCE*, Vol. 10, Num. 7, (July 2005) pp. 49-57.

Lanceros-Me ndez, S., Mano, J. F., Costa. A. M. (2001) FTIR AND DSC STUDIES OF MECHANICALLY DEFORMED B-PVDF FILMS, *Macromolecular Science: Physics*, Vol. B40, No. 3&4, pp. 517-527, ISSN 0022-2348.

Lbonard, C., Halary, J. L., & Monnerie, L., (1988), Crystallization of poly(vinylidene fluoride)-poly(methyl methacrylate) blends: analysis of the molecular parameters controlling the nature of poly(vinylidene fluoride) crystalline phase, *Macromolecules*, Vol: 21, No. 10, (October 1998) pp. 2988-2994, ISSN 0024-9297.

Lovinger, A., (1982) Annealing of poly(vinylidene fluoride) and formation of a fifth phase, *Macromolecules,* Vol. 15, No. 1, pp. 40-44, ISSN 0024-9297.

Matsushige, K., Nagata, K., Imada, S., & Takemura. T., (1980) The II-I crystal transformation of poly(vinylidene fluoride) under tensile and compressional stresses, *Polymer*, Vol. 21, No. 12, (October 1979), PP. 1391-1397, ISSN 0032-3861.

Mattsson, B., Ericson, H., Torell, L. M., Sundholm. F., (1999) Micro-Raman Investigations of PVDF-Based Proton-Conducting Membranes. *Polymer Science Part A: Polymer Chemistry,* Vol. 37, pp.3317-3327, ISSN 1099-0518.

Miller, R. L., Raisoni,. J. J., (1976) Single crystals of poly(vinylidene fluoride), Polymer science polymer physics, Vol. 14, No. 12 (March 2003), pp. 2325-2326, ISSN 1099-0518.

Mohamadi, S., Sharifi-Sanjani, N. & Mahdavi. H., (2011) Functionalization of Graphene Sheets via Chemically

Mohamadi. S., & Sharifi-Sanjani, N., (2011) Investigation of the crystalline structure of PVDF in PVDF/PMMA/Graphene polymer blend nanocomposites, Polymer Composites, Vol. 32, pp. 1451–1460, ISSN 0272-8397.

Nalwa. N. S., (1995) *Ferroelectric Polymers*, Marcel Dekker, NewYork , INC, ISBN 0-8247-9468-0.

Ogoshi, T., & Chujo, Y., (2005) Synthesis of poly(vinylidene fluoride) (PVdF)/silica hybrids having interpenetrating polymer network structure by using crystallization between PVdF chains, Polymer Science: Part A, Polymer Chemistry, Vol. 43, No. 16, pp. 3543-3550, ISSN 1099-0518.

Park, Y. J., Kang , Y. S., Park. C. (2005) Micropatterning of semicrystalline poly(vinylidene fluoride) (PVDF) solutions, European Polymer Journal, Vol. 41, pp. 1002–1012, ISSN 0014-3057.

Potts, J. R., Dreyer, D. R., Bielawski, C. W., Ruoff. R. S., (2011), Graphene-based polymer nanocomposites, Polymer, Vol. 53, No. 1, (November 2010), pp. 5-25, ISSN 0032-3861.

Pramoda, K. P., Linh, N.T.T. , Tang , P.S. , Tjiu, W.C. , Goh, S. H., He. C.B. , (2010) Thermo-mechanical properties of poly(vinylidene fluoride) modified graphite/poly(methyl methacrylate) nano composites, *Composite Science and Technlogy,* Vol. 70, No. 4,( December 2009) pp. 578-583, ISSN 0266-3538.

Pramoda, K., Mohamed, A., Phang, I. Y., & Liu. T., (2005) Crystal transformation and thermomechanical properties of poly(vinylidene fluoride)/clay nanocomposites, *Polymer International*, Vol. 54, No. 1, (April 2004)pp. 226-232, ISSN 1097-0126.

Ramanathan, T., Stankovich, S., Dikin, D. A., Liu, H., Shen, H., Nguyen, S. T., & Brinson. L. C., (2007), Graphitic nanofillers in PMMA nanocomposites—An investigation of particle size and dispersion and their influence on nanocomposite properties, Polymer Science : Part B: Polymer Physics, Vol. 45, No. 15, pp. 2097-2112, ISSN 1099-0488.

Ramasundaram, S., Yoon, S., Kim, K. J. , Park. C., (2008). Preferential Formation of Electroactive Crystalline Phases in Poly(vinylidene fluoride)/Organically Modified Silicate Nanocomposites, Polymer science: Part B: Polymer Physics, Vol. 46, 2173–2187, ISSN 1099-0518.

Scheinbeim, J. I., Newman, B. A., Sen. A., (1986), Field-induced crystallization in highly plasticized poly(vinylidene fluoride) films, *Macromolecules*, Vol. 19 (November, 1985), PP. 1454-1458. ISSN 0024-9297.

Stankovich, S., Dikin, D. A., Dommett, G. H. B., Kohlhaas, K. M., Zimney, E. J., Stach, E. A., & Piner, R. D. (2006) Graphene-based composite materials, *Nature*, Vol, 442, pp. 282-286, ISSN 0028-0836.

Stankovich, S., Dikin, D. A., Piner, R. D., Kohlhaas, K. A., Kleinhammes, A., Jia, Y., Wu, Y., Nguyen, S. T., & Ruoff, R. S. (2007) Synthesis of graphene-based nanosheets via chemical reduction of exfoliated graphite oxide , *Carbon*, Vol. 45, pp. 1558-1565, ISSN 0008-6223.

Steurer, P., Wissert, R., Thomann, R., & Mülhaupt. R. (2009) Functionalized Graphenes and Thermoplastic Nanocomposites Based upon Expanded Graphite Oxide, *Macromolecular Rapid Communication*, Vol. 30, No. 4-5. pp. 316-327, ISSN 1521-3927.

Steurer. P., Wissert, R., Thomann, R., Mülhaupt. R., (2009), Functionalized Graphenes and Thermoplastic Nanocomposites Based upon Expanded Graphite Oxide, *Macromolecular Rapid Communication*. Vol. 30, pp. 316–327, ISNN 1521-3927.

Ulaganathan, M., & Rajendran, S. ( 2010) Preparation and characterizations of PVAc/P(VdF-HFP)-basedpolymer blend electrolytes, Ionics, Vol. 16, (December 2009) pp. 515-521, ISSN 0947-7047.

Vo, L. T., & Giannelis. E. P., (2007) Compatibilizing Poly(vinylidene fluoride)/Nylon-6 Blends with Nanoclay. J. Macromolecules, Vol. 41, No. 23( August , 2007) pp. 8271-8226, ISSN 0024-9297.

Wang, J., Li, H., Liu, J., Duan, Y., Jiang, S., Yan. S., (2003), On the α → β Transition of Carbon-Coated Highly Oriented PVDF Ultrathin Film Induced by Melt Recrystallization, *Journal of American chemical society*, Vol. 125, No. 6, (November, 2002) pp. 1496-1497, ISSN 0002-7863.

Yang, D., & Chen. Y., (1987), β-phase formation of poly(vinylidene fluoride) from the melt induced by quenching, *Journal of material science letter*, Vol. 6, No. 5, pp. 599-603, ISSN 0261-8028.

Yee, W. A., Kotaki, M., Liu, Y., Lu. X., (2007) Stress-induced structural changes in electrospun polyvinylidene difluoride nanofibers collected using a modified rotating disk, *Polymer*, Vol. 49, No. 19, pp. 4196-4203, ISSN 0032-3861.

Yen, J. H., Amin-Sanayei, R., (2006). Polyvinylidene Fluoride, in: *Encyclopedia of Chemical Processing,Vol.1,* Lee. S, pp. (2379-2381), Tailor & Francis, ISBN 9780824755003, New York.

Yu, L., & Cebe. P., (2009) Effect of nanoclay on relaxation of poly(vinylidene fluoride) nanocomposites, Journal of Polymer Science: Part B: Polymer Physics, Vol. 47, No. 24, (August 2009) pp. 2520–2532, ISSN 1099-0518.

Yu, S., Zheng, W., Yu, W., Zhang, Y., Jiang, Q., & Zhao. Z., (2009) Formation Mechanism of β-Phase in PVDF/CNT Composite Prepared by the Sonication Method, *Macromolecules,* Vol. 42, No. 22, pp. 8870, ISSN 0024-9297.

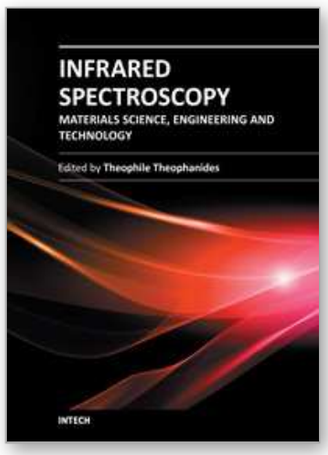


**Infrared Spectroscopy - Materials Science, Engineering and Technology**

Edited by Prof. Theophanides Theophile

ISBN 978-953-51-0537-4
Hard cover, 510 pages
**Publisher** InTech
**Published online** 25, April, 2012
**Published in print edition** April, 2012

The present book is a definitive review in the field of Infrared (IR) and Near Infrared (NIR) Spectroscopies, which are powerful, non invasive imaging techniques. This book brings together multidisciplinary chapters written by leading authorities in the area. The book provides a thorough overview of progress in the field of applications of IR and NIR spectroscopy in Materials Science, Engineering and Technology. Through a presentation of diverse applications, this book aims at bridging various disciplines and provides a platform for collaborations among scientists.

**How to reference**

In order to correctly reference this scholarly work, feel free to copy and paste the following:

Somayeh Mohamadi (2012). Preparation and Characterization of PVDF/PMMA/Graphene Polymer Blend Nanocomposites by Using ATR-FTIR Technique, Infrared Spectroscopy - Materials Science, Engineering and Technology, Prof. Theophanides Theophile (Ed.), ISBN: 978-953-51-0537-4, InTech, Available from: http://www.intechopen.com/books/infrared-spectroscopy-materials-science-engineering-and-technology/preparation-and-characterization-of-pvdf-pmma-graphene-polymer-blend-nanocomposites-by-using-ft-ir-t

INTECH
open science | open minds

**InTech Europe**
University Campus STeP Ri
Slavka Krautzeka 83/A
51000 Rijeka, Croatia
Phone: +385 (51) 770 447
Fax: +385 (51) 686 166
www.intechopen.com

**InTech China**
Unit 405, Office Block, Hotel Equatorial Shanghai
No.65, Yan An Road (West), Shanghai, 200040, China
中国上海市延安西路65号上海国际贵都大饭店办公楼405单元
Phone: +86-21-62489820
Fax: +86-21-62489821

IntechOpen